Bull Yamaguchi Med Sch 46(3-4) : 83-91, 2000

Clinical Application of Gadolinium-Enhanced Three-Dimensional Pulmonary MR Angiography

Katsuyuki Takano

Department of Radiology, Yamaguchi University School of Medicine1-1-1, Minamikogushi, Ube, Yamaguchi 755-8505, JAPAN.
(Received October 20, 1999, revised December 22, 1999)

Abstract Twenty-nine patients with suspected pulmonary lesions, and three normal volunteers, underwent gadolinium-enhanced three-dimensional (3D) pulmonary MR angiography (MRA). The MRA were obtained during intravenous administration of gadolinium-based contrast material, in a single breath-hold. Conspicuity of the normal pulmonary segmental arteries was estimated on the MRA. Abnormal findings such as "vascular involvement", "abnormal connection", "stenosis", or "dilatation" on the MRA were compared with those on conventional angiography or CT. Normal pulmonary segmental arteries, except for $A^{4,5,6,8,and9}$ of the left pulmonary artery, could be clearly visualized. Blind reading of four different findings lead to characteristic findings for each pulmonary disease that can be aid in their differential diagnoses. This technique shows promise as a noninvasive diagnosis of lung diseases.

Key Words: pulmonary diseases, 3D MRA, gadolinium-enhancement

Introduction

Though conventional pulmonary angiography is considered a standard of reference for diagnosing pulmonary vascular disorders, clinical applications of MR angiography (MRA) have been documented for pulmonary vasculatures [1-5]. Conventional angiography is an invasive technique, which can not be easily performed in patients with pulmonary hypertension or a past history of allergy to iodinated agents. Gadopentetate dimeglumine (Gd-DTPA) is an effective intravenous paramagnetic contrast agent that has little measurable toxicity at imaging doses [6,7].

In the present study, MR sequence is based on breath-hold 3D data acquisition, and intravenous administration of paramagnetic contrast agents. It has been reported that 3D pulmonary MRA might be superior to 2D pulmonary MR angiography [8]. Paramagnetic contrast agents can increase signal intensity of the pulmonary arteries especially in the 3 D gradient-echo technique. Then, susceptibility of artifacts due to the presence of the alveolar air-tissue interface is one of significant problems in MR imaging of the thorax. The tradeoff, in reducing susceptible artifacts by shortening echo time (TE) and readout bandwidth, must also be considered. Shorter TE will considerably reduce susceptible artifacts and intravoxel dephasing in 3D gradient-echo imaging[9]. Moreover, a shorter TE helps in shortening repetition time (TR) which makes the breath-hold technique possible by reducing acquisition time. However, a shorter TR can reduce the time of flight (TOF) effect due to a decrease in the T1 relaxation time of spin saturation in the blood. Thus, administration of a paramagnetic contrast agent becomes indispensable in 3D TOF MRA.

The use of a phased-array coil improves the

signal-to-noise ratio (S/N) and in particular makes peripheral vessels more clearly defined on MR imaging[10,11]. Fast gradient-echo angiographic sequences were used to provide excellent spatial and temporal resolutions of the pulmonary vasculatures. The purpose of this study was to evaluate visualizations of the pulmonary arteries with gadolinium-enhanced 3D MRA using fast gradient-echo sequence and a phased-array coil.

Subjects and Methods

MR image technique

MRA was performed with a phased-array coil on a superconducting MR unit operating at 1.5-T (MAGNETOM Vision SIEMENS Medical Systems: Erlangen, Germany) with a 25-m Tesla/m maximum gradient amplitude. The pulse sequence was 3D fast gradient-echo technique without ECG gating. Source images were obtained in the coronal plane using a fast imaging with steady-state free precession (FISP) technique with a shorter TR and TE: a TR of 5.0 msec, TE of 2.0 msec, flip angle of 10 degree, field of view (FOV) of 380 mm, slab thickness of 78~84mm (26~28 partitions), an acquisition matrix of 154×256, and one acquisition. To obtain the maximum signal intensity of the pulmonary artery, the imaging start time needs to be determined from when the center row in k-space is filled on the first pass of contrast material to the pulmonary artery.

The signal intensity of the pulmonary artery became relatively high, when the center row of k-space was filled, 10-20 sec after intravenous injection of paramagnetic contrast administration. The ideal time then, from the injection of contrast agent to the center of the MRA scan, must be about 15sec [4]. The acquisition time was 26 sec using the FISP technique; therefore the MRA scan was started as soon as the injection of Gd-DTPA (0.1mmol/kg, 3ml/sec.) was finished. After all data was collected, each source image was reviewed and postprocessed using maximum intensity projection (MIP) algorithms, with rotating projection angles every 20 degrees in the anteroposterior direction.

Study group

This study began with 3 volunteers, and 29 patients with suspected lung diseases. Breath hold was not successful in nine of the 29 patients. All examinations were performed between May and December 1998. Lung diseases in the 29 patients (nineteen men, ten women) from 23 to 78 years of age (mean age, 54 years) were as follows: lung cancer (n=19), pulmonary arteriovenous fistula (n=4), pulmonary thromboembolism (n=3), primary pulmonary hypertension (n=3).

The MRA findings of the three normal volunteers were used to evaluate the detectability and conspicuity of normal pulmonary segmental branches. In addition to this analysis of normal pulmonary branches, the diagnostic ability of MRA in pulmonary vascular diseases was evaluated in the 20 of the 29 patients who had confirmatory examinations for final diagnosis including chest CT and/or conventional pulmonary angiography.

Normal image analysis

Conspicuity of the normal pulmonary segmental branches was extensively evaluated in 51 normal lung segments of the three normal volunteers by two radiologists, and in the absent side of vascular abnormalities in the 9 successful breath-hold patients.

Conspicuity was determined in each segment using a 4-point scale: 4 = a segmental pulmonary artery was totally visualized, 3 = a segmental pulmonary artery was totally visualized, but its image was degraded by artifacts, 2 = a segmental pulmonary artery was partially visualized, 1 = a segmental pulmonary artery was not visualized. To assess inter-observer variability, for the assignment of a confidence level to the conspicuity of pulmonary segmental arteries, a weighted κ statistic was calculated [12]. The level of agreement was defined as follows: κ values of less than 0 indicated no agreement; κ values of 0.00-0.40 indicated poor agreement; κ values of 0.41-0.75 represented good agreement; κ values of 0.76-1.00 represented excellent agreement.

Clinical image analysis

MR angiograms were independently interpreted by three radiologists who had no

knowledge of the findings on other procedures. MR images in 20 patients who underwent CT (19 patients) and conventional pulmonary angiography (six patients) were reviewed to evaluate the diagnostic ability of MRA in pulmonary vascular disorders. The presence of the following MRA findings were assessed: "vascular involvement", "abnormal connection", "stenosis", and "dilatation". "Vascular involvement" was considered present when peripheral pulmonary arteries were involved in the lung cancer. "Abnormal connection" was suggested by an aberrant origin of the pulmonary arteries or "abnormal connection" between the pulmonary arteries and the veins. "Stenosis" was considered present when an intraluminal signal defect was seen in the proximal pulmonary arteries. "Dilatation" was considered present when the pulmonary arteries were increased in diameter.

In addition, the confidence level for each finding was rated to calculate the accuracy of a confident diagnosis. The confidence level of each finding was determined using a 4-point score: 4 = the relevant abnormal vessels were clearly defined, 3 = the relevant abnormal vessels were visualized, but their images were degraded by artifacts, 2 = the abnormal vessels were thought to exist, but the abnormality type was unknown, 1 = the abnormal vessels were not visualized. A score of 3 or 4 was considered as indicating positive findings.

Results

In normal image analysis, visualization of the pulmonary segmental arteries was summarized on a successful breath hold (Table 1). The pulmonary segmental arteries were satisfactorily visualized (mean score of 3 or more) in most segments with good interobserver agreement (the weighted κ values; 0.62), except for $A^{4,5,6,8,and9}$ of the left pulmonary artery. Two readers graded the conspicuity of $A^{4,5,6,8,and9}$ of the left pulmonary artery less than 3.00 point. Poor conspicuity of the pulmonary segment arteries existed in the left upper-lower and lower lobes. Especially in $S^{4,5}$ of the left pulmonary segment adjacent to the heart, the pulmonary arteries could not be clearly visualized. Unsuccessful breath-

Table 1. Mean score for conspicuity of segmental pulmonary arteries

Note. — Data is a mean score for conspicuity of each of three pulmonary segmental arteries.

Pulmonary Artery Segment	Reader 1	Reader 2
Right A^1	3.33	3.67
Right A^2	3.67	4.00
Right A^3	3.67	3.67
Right A^4	3.33	3.67
Right A^5	3.00	3.33
Right A^6	3.33	3.33
Right A^8	3.00	2.33
Right A^9	3.00	3.33
Right A^{10}	3.00	3.00
Left A^{1+2}	3.00	3.33
Left A^3	3.33	3.33
Left A^4	2.33	2.33
Left A^5	2.67	2.00
Left A^6	2.33	2.67
Left A^8	2.67	2.33
Left A^9	2.33	2.67
Left A^{10}	2.33	3.00

Table 2. True positive and negative rates for four findings on source images and MIP images of MRA Data is in percentages.

Clinical findings (n: Positive number found)	Source images Mean score of true positive rate	MIP images Mean score of true positive rate	Source images Mean score of true negative rate	MIP images Mean score of true negative rate
Vascular involvement (n=7)	0.96	0.81	1.00	1.00
Stenosis (n=9)	1.00	0.56	1.00	1.00
Abnormal connection (n=4)	0.93	0.68	1.00	1.00
Dilatation (n=7)	1.00	1.00	1.00	1.00

holding resulted in an increase of ghosting artifacts, and the score was less than 2.00 point in each pulmonary segmental artery.

In clinical image analysis, the MRA findings of the source image had a good relationship with those of CT or conventional angiography (Table 2). "Dilatation" was common on source and MIP images in all patients with pulmonary arteriovenous fistula (Fig. 1) and primary pulmonary hypertension (Fig. 2). Detectability of "dilatation" was almost equal to that on CT or conventional angiography. "Vascular involvement" was seen with a 96% true positive rate on source images and with an 81% true positive rate on MIP images. "Stenosis" was seen on source images with a 100% true positive rate and on MIP images with a 68% true positive rate. "Abnormal connection" was seen on source images with a 93% true positive rate and on MIP images

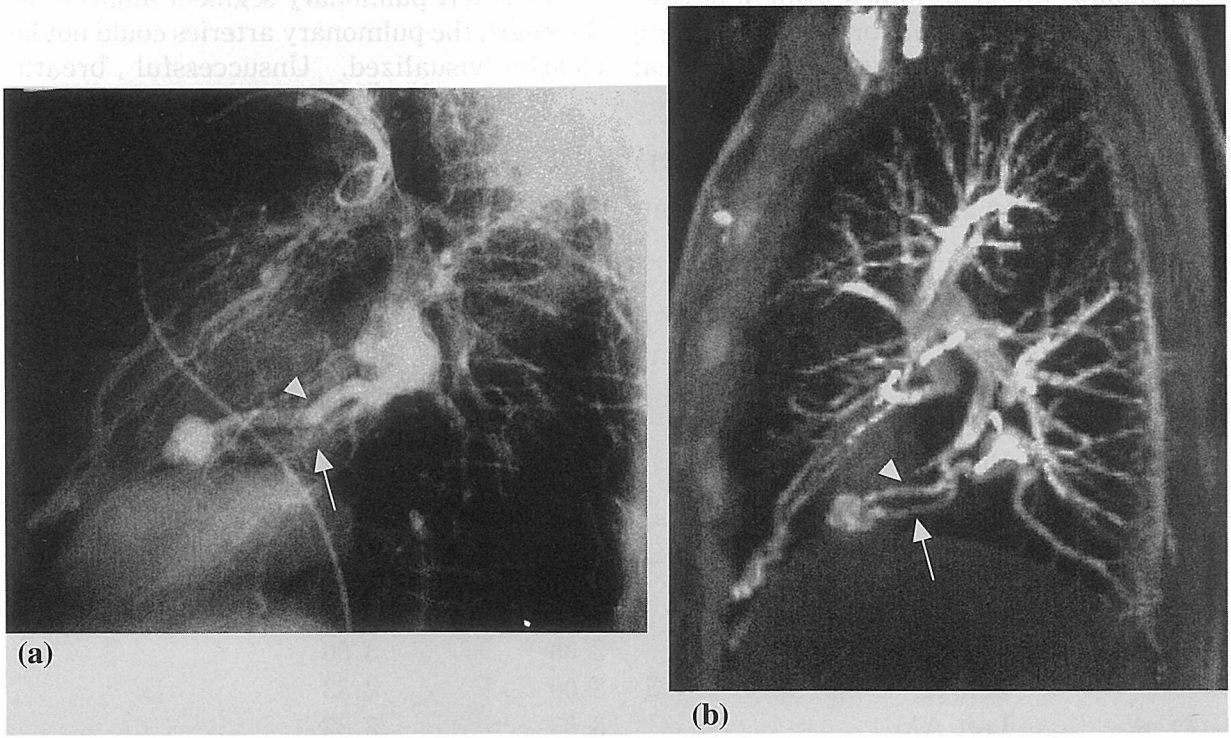

Fig 1. Pulmonary arteriovenous fistula in a 63-year-old woman.
(a) Conventional pulmonary angiogram shows the anomalous communication between the pulmonary artery (arrow) and pulmonary vein (arrowhead), but these vessels are not clearly separated from each other.
(b) MIP image of pulmonary MRA also demonstrates the pulmonary arteriovenous fistula in $S^{8}b$ of the right pulmonary segment (arrow: the pulmonary artery, arrowhead: the pulmonary vein).

with a 68% true positive rate. Source images were superior to MIP images in detecting "vascular involvement", "stenosis" and "abnormal connection". True negative rates were 100% in all four findings on both MRA images.

Data shows blind reading of each pulmonary disease on the source images of MRA, compared with CT or conventional angiography as the gold standard (Table 3). "Stenosis" of the pulmonary arteries was seen in 67% of the 7 patients with lung cancer on MRA, CT, and conventional angiography. Lung cancer was subtracted on digital subtraction angiography (Fig. 3), but the spatial relationship between lung cancer and the pulmonary vessels could not be evaluated in two patients. In pulmonary arteriovenous fistula, "abnormal connection" and "dilatation" of the pulmo nary artery were clearly shown in all four patients on all three procedures (Fig. 1). In all three patients with pulmonary thromboembolism, "stenosis" of the pulmonary artery was seen on MRA. Intraluminal thrombus was clearly shown as a hypointense structure compared to the signal intensity of normal lumen on MRA. "Dilatation" of the pulmonary trunk was seen in all three patients with primary pulmonary hypertension on MRA.

On MIP images, visibility of the thrombus of the pulmonary artery decreased in two patients (Fig. 4). The ability of making a confident diagnosis for pulmonary diseases was compared between MIP and source images. A confident diagnosis of "stenosis" (rating of 3 or 4) was rendered in four (40%) patients on MIP, while it was rendered in six (60%) patients on source images among the 10 patients with lung cancer. "Abnormal connection" was shown in 68% patients on MIP, and in 93% on source images among the four patients with pulmonary arteriovenous fistula. "Stenosis" was shown in one (33.3%) patient on MIP, and in three (100%) patients on source image among the three patients with pulmonary thromboembolism. These results indicate the superiority of source images in diagnosis of each pulmonary dis-

Table 3. Clinical findings of lung diseases on MRA (source images and MIP images), and CT or conventional angiography
*Vascular involvement was diagnosed on CT (7/10) and angiography (5/10).

Clinical diagnosis	Positive findings	Mean number of cases on MRA		CT or conventional angiography
		Source images	MIP images	
Lung cancer (n=10)	Vascular involvement	6.7/10.0	5.7/10.0	*7.0/10.0
	Abnormal connection	0.0/10.0	0.0/10.0	0.0/10.0
	Stenosis	6.0/10.0	4.0/10.0	6.0/10.0
	Dilatation	0.0/10.0	0.0/10.0	0.0/10.0
Pulmonary arteriovenous fistula (n=4)	Vascular involvement	0.0/4.0	0.0/4.0	0.0/4.0
	Abnormal connection	3.7/4.0	2.7/4.0	4.0/4.0
	Stenosis	0.0/4.0	0.0/4.0	0.0/4.0
	Dilatation	4.0/4.0	4.0/4.0	4.0/4.0
Pulmonary thromboembolism (n=3)	Vascular involvement	0.0/3.0	0.0/3.0	0.0/3.0
	Abnormal connection	0.0/3.0	0.0/3.0	0.0/3.0
	Stenosis	3.0/3.0	1.0/3.0	3.0/3.0
	Dilatation	0.0/3.0	0.0/3.0	0.0/3.0
Primary pulmonary hypertension (n=3)	Vascular involvement	0.0/3.0	0.0/3.0	0.0/3.0
	Abnormal connection	0.0/3.0	0.0/3.0	0.0/3.0
	Stenosis	0.0/3.0	0.0/3.0	0.0/3.0
	Dilatation	3.0/3.0	3.0/3.0	3.0/3.0

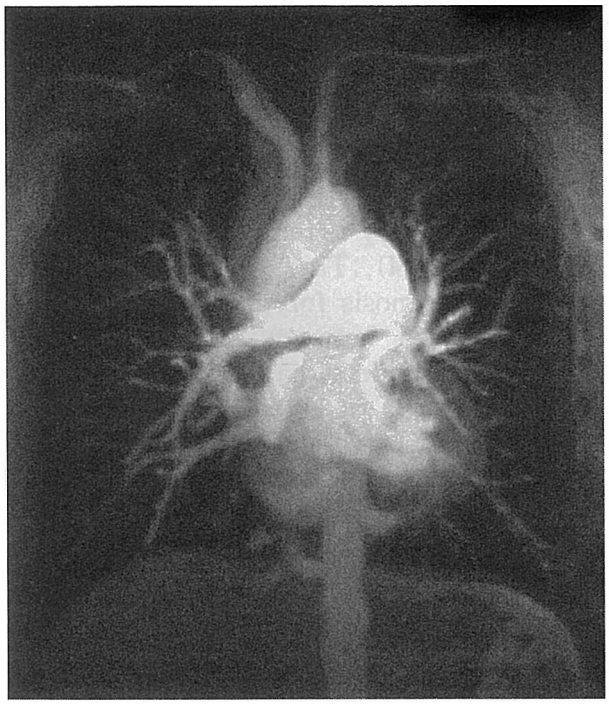

Fig 2. Primary pulmonary hypertension in a 70-year-old man. The dilatation of the proximal pulmonary arteries and tapering of the peripheral pulmonary arteries is clearly visualized on the MIP image of MRA.

ease (Table 3).

Discussion

Hatabu et al.[13] in 1992 used gradient recalled acquisition in a steady state with breath-hold technique and dual surface coils, but without injection of paramagnetic contrast materials. They mentioned that six- and seventh-order branches could be visualized, especially near the coils on the single-section axial image obtained. However, the pulmonary vessels far from the coils could not be clearly visualized because of lower signal intensity.

In the present study, MRA study with the injection of paramagnetic contrast materials was demonstrated using a newly developed phased-array coil covering the overall thorax. The peripheral and proximal pulmonary vessels can be constantly seen down to the six-and seventh-order branches in successful breath-holding, except in the left upper- lower and lower lobes. Especially, the proximal pulmonary arteries are clearly visualized, as well as the peripheral pulmonary arteries adjacent to received coil are. In our study, the peripheral and proximal pulmonary arteries were more clearly visualized by adding the

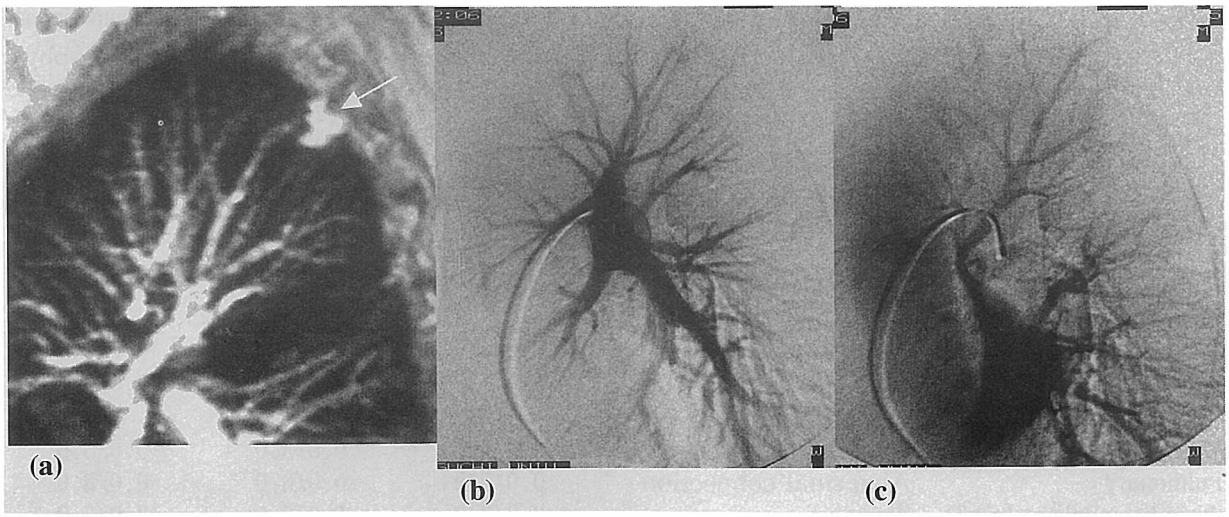

Fig 3. Lung cancer in a 67-year-old man.
(a) In the targeted MIP image, the spatial relationship between the lung cancer (arrow) and the pulmonary vessels can be easily recognized.
(b, c) In pulmonary arterial phase (b) and venous phase (c) of DSA, the lung cancer in S^2b of the right pulmonary segment is subtracted, and A^2b of the right pulmonary artery and V^2b of the right pulmonary vein alone are visible.

use of a phased body-array coil and administration of Gd-DTPA, than by not using these. It is thought that gadolinium-enhanced 3D MRA may be one of the most useful noninvasive techniques for delineating pulmonary vasculatures.

There were no statistically significant differences in the conspicuity of the pulmonary segmental arteries by the two inter-observers (Table 1). The pulmonary segmental arteries, except for $A^{4,5,6,8,and9}$ of the left pulmonary artery, were satisfactorily visualized with mean score of 3 or more, suggesting that this technique will increase confidence for detecting and evaluating pulmonary vasculatures. These results confirm that gadolinium-enhanced 3D MRA affords us reliable information of the pulmonary arteries.

The image quality was degraded by MIP reconstruction in the detection of "vascular involvement", "stenosis", and "abnormal connection" (Table 2). Especially, the ability of a confident diagnosis of "stenosis" was higher in source images than that in MIP images, because "stenosis" of the targeted pulmonary arteries was missed due to the overlapping with major vessels or the heart on MIP images. Whereas MIP is a good method as post-processing method, careful reading of source images is necessary for an accurate diagnosis in a pulmonary MRA study. There was no statistically significant difference in detecting "dilatation" on both MR images.

In the clinical study, blind reading of four different findings lead to characteristic findings for each disease, which can aid in their differential diagnoses (Table 3). On source images, "abnormal connection" and "dilatation" of the clinical findings are seen in all patients with pulmonary arteriovenous fistula and primary pulmonary hypertension, and are diagnostic for them. Diagnostic ability of MRA in detecting "abnormal connection" and "dilatation" was nearly equal to CT or DSA. The presence or absence of "vascular involvement" was important in differentiating peripheral lung cancer from benign nodules. In our study, MRA demonstrated the relationship of the pulmonary artery and mass, which was missed by DSA, because lung cancer was subtracted in DSA. However, confident agreement of "vascular involvement" on MRA was superior to that on CT. The presence of "stenosis" suggests vascular invasion in lung cancer, and pulmonary arterial thrombus in pulmonary thromboembolism. On source images, "stenosis" in pulmonary thromboembolism was detected with confident agreement, whereas "stenosis" in lung cancer was not clearly visualized than that in pulmonary

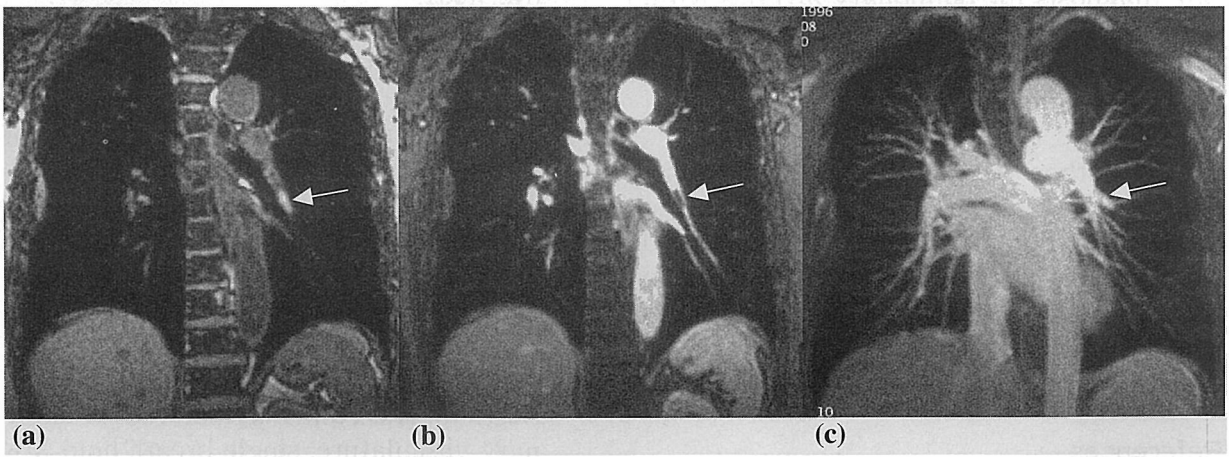

Fig 4. Pulmonary thromboembolism in a 39-year-old man.
(a) The source image of unenhanced pulmonary MRA shows a hyperintense lesion suggesting pulmonary embolus (arrow) in the left pulmonary artery.
(b) In the dynamic study, the lesion is revealed as a hypointense lesion (arrow) compared to the signal intensity of the normal lumen in the dynamic pulmonary MRA.
(c) In the MIP image of the pulmonary MRA, the embolus is missed due to overlapping of the other pulmonary vessels (arrow).

thromboembolism. These results suggested that excellent spatial resolution is needed in clinical diagnosis of lung cancer. So, it is concerned that more spatial resolution is needed on MRA in diagnosis of "stenosis" in lung cancer.

This study has some limitations. First, successful breath-hold is necessary for obtaining clear images of pulmonary vasculatures. Unsuccessful breath-holding also resulted in an increase of ghosting artifacts, which degrades the MRA image quality. Ghosting artifacts are eventually an important problem, particularly in MIP reconstruction. Nevertheless, most of pulmonary peripheral vessels can be clearly visualized in successful breath holding. Second, the ghosting artifacts, due to cardiac motion occurring among the phase-encoding direction, degraded MR image quality of the pulmonary vascular disorders. So, the conspicuity of pulmonary segmental visualization in the area adjacent to the heart was inferior to that in other areas. ECG-gating is necessary for reducing artifacts due to cardiac motion.

In the summary, gadolinium-enhanced 3D MRA has a potential to delineate normal pulmonary segmental branches, and to demonstrate characteristic findings for each pulmonary disease, which can aid in their differential diagnoses. This technique allows accurate diagnosis for pulmonary arteries within a reasonable measurement time.

Acknowledgements

The author wishes to thank Professor Naofumi Matsunaga, Department of Radiology, Yamaguchi University School of Medicine, for his excellent advice in completing this manuscript, and Tsuneo Matsumoto, Gouji Miura, Katsuyoshi Ito, Nobuyuki Tanaka, for expert interpretation of MRA images.

References

1) Wieloplski P.A., Haacke E.M., and Adler L.P. : Three-dimensional MR imaging of the pulmonary vasculature: preliminary experience. *Radiology*, **183** : 465-472, 1992.
2) Doyle A.J. : Demonstration of blood supply to pulmonary sequestration by MR angiography. *Am J Roentgenol,* **158** : 989-990, 1992.
3) Loubeyre P., Revel D., Douek P. Delignette A., Baldy C., Genin G., and Amiel M.: Dynamic contrast-enhanced MR angiography of pulmonary embolism: comparison with pulmonary angiography. *Am J Roentgenol,* **162** : 1035-1039, 1994.
4) Isoda H., Ushimi T., Masui T., Mochizuki T., Goto S., Suzuki K., Shirakawa T., Ohta A., Takahashi M., and Kaneko M. : Clinical evaluation of pulmonary 3D time-of-flight MRA with breath holding using contrast media. *J Comput Assist Tomogr,* **19** : 911-919, 1995.
5) Meaney J.F.M., Weg J.G., Chenevert T.L., Stafford-Johnson D., Hamilton B.H., and Prince M.R. : Diagnosis of pulmonary embolism with magnetic resonance angiography. *N Engl J Med,* **336** : 1422-1427, 1997.
6) Weinmann H.C., Brasch R.C., Press W.R., and Wesbey G.E. : Characteristic of gadolinium-DTPA complex: a potential NMR contrast agent. *Am J Roentgenol,* **142** : 619-24, 1984.
7) Bergin C.J., Glover G.H., and Pauly J.M. : Lung parenchyma: magnetic susceptibility in MR imaging. *Radiology,* **180** : 845-848, 1991.
8) Isoda H., Masui T., Hasegawa S., Shirakawa T., Ohta A., Takahashi M., and Kaneko M. : Pulmonary MR angiography: a comparison of 2D and 3D time of flight. *J Comput Assist Tomogr,* **18** : 402-407, 1994.
9) Haacke E.M., Tkach J.A., and Parrish T. B. : Reduction of T2* dephasing in gradient field-echo imaging. *Radiology,* **170** : 457-462, 1989.
10) Foo T.K.F., MacFall J.R., Hayes C.E., Sostman H.D., and Slayman B.E. : Pulmonary vasculature: single breath-hold MR imaging with phased-array coils. *Radiology,* **183** : 473-477, 1992.
11) Hatabu H., Gefter W.B., Listerud J., Hoffman E.A., Axel L., McGowanIII J.C., Palevsky H.I., Hayes C.E., Konishi J., and Kressel H.Y. : Pulmonary MR angiography utilizing phased-array surface coils. *J*

Comput Assist Tomogr, **16** : 410-7, 1992.
12) Fleiss J.L. : The measurement of inter-rater agreement. In: Statical methods for rates and proportions. 2*nd ed. New York, NY: Wiley,* 212-236, 1981.
13) Hatabu H., Gefter W.B., Kressel H.Y., Axel L., and Lenkinski R.E. : Pulmonary vasculature: high-resolution MR imaging. *Radiology,* **171** : 391-395, 1989.